Published for SISSA by Springer

Received: October 4, 2019
Accepted: November 19, 2019
Published: December 2, 2019

ΔM_s theory precision confronts flavour anomalies

Luca Di Luzio,[a] **Matthew Kirk,**[b] **Alexander Lenz**[c] **and Thomas Rauh**[d]

[a] *Dipartimento di Fisica "E. Fermi", Università di Pisa and INFN Sezione di Pisa, Largo Bruno Pontecorvo 3, I-56127 Pisa, Italy*

[b] *Dipartimento di Fisica, Università di Roma "La Sapienza", and INFN Sezione di Roma, Piazzale Aldo Moro 2, 00185 Roma, Italy*

[c] *Institute for Particle Physics Phenomenology, Durham University, DH1 3LE Durham, United Kingdom*

[d] *Albert Einstein Center for Fundamental Physics, Institute for Theoretical Physics, University of Bern, Sidlerstrasse 5, CH-3012 Bern, Switzerland*

E-mail: luca.diluzio@pi.infn.it, matthew.kirk@roma1.infn.it, alexander.lenz@durham.ac.uk, rauh@itp.unibe.ch

Abstract: Based on recent HQET sum rule and lattice calculations we present updated Standard Model predictions for the mass differences of neutral B mesons: $\Delta M_s^{\rm SM} = \left(18.4^{+0.7}_{-1.2}\right) \text{ps}^{-1}$ and $\Delta M_d^{\rm SM} = \left(0.533^{+0.022}_{-0.036}\right) \text{ps}^{-1}$ and study their impact on new physics models that address the present hints of anomalous data in $b \to s\ell\ell$ transitions. We also examine future prospects of further reducing the theory uncertainties and discuss the implications of a 2025 scenario with $\Delta M_s^{\rm SM\ 2025} = (18.4 \pm 0.5)\,\text{ps}^{-1}$. In particular, the latter yields upper bounds $M_{Z'} \lesssim 9\,\text{TeV}$ and $M_{S_3} \lesssim 30\,\text{TeV}$ for the minimal Z' and S_3 lepto-quark explanations of the $b \to s\ell\ell$ anomalies, respectively.

Keywords: Beyond Standard Model, CP violation, Heavy Quark Physics

ArXiv ePrint: 1909.11087

https://doi.org/10.1007/JHEP12(2019)009

Contents

JHEP12(2019)009

1 Introduction

The mixing of neutral B mesons provides an important test of our understanding of the Standard Model (SM). It gives direct access to the poorly known CKM elements V_{td}, V_{ts} and V_{tb}, and it is an excellent probe for physics beyond the standard model (BSM), see e.g. [1].

By now the experimental values of the mass differences of the neutral B mesons are known very precisely [2] (based on the measurements in [3–10])

$$\Delta M_d^{\text{exp}} = (0.5064 \pm 0.0019)\,\text{ps}^{-1}\,, \tag{1.1}$$

$$\Delta M_s^{\text{exp}} = (17.757 \pm 0.021)\,\text{ps}^{-1}\,. \tag{1.2}$$

The theoretical determination of the mass differences is limited by our understanding of non-perturbative matrix elements of dimension six operators. The matrix elements can be determined with lattice simulations or sum rules. Both approaches utilize a three-point correlator of two interpolating currents for the B_q and $\bar{B}_q$ mesons and the dimension six operator, which is significantly more complicated than the determination of decay constants where one considers a two-point correlator of two currents. Therefore, for a long time (see e.g. the FLAG 2013 review [11]) the precision of the matrix elements was limited to more

than 10%. The consequence were SM predictions of ΔM_q [1] close to the experimental numbers, but with much higher uncertainties:

$$\Delta M_d^{\text{FLAG 2013}} = (0.528 \pm 0.078)\,\text{ps}^{-1} = (1.04 \pm 0.15)\,\Delta M_d^{\text{exp}}\,, \tag{1.3}$$

$$\Delta M_s^{\text{FLAG 2013}} = (18.3 \pm 2.7)\,\text{ps}^{-1} = (1.03 \pm 0.15)\,\Delta M_s^{\text{exp}}\,. \tag{1.4}$$

In 2016 [12] the FNAL/MILC collaboration presented a new evaluation of the non-perturbative B mixing matrix elements yielding larger values than previously obtained. They achieved relative errors of 8.5% and 6.4% for the matrix elements relevant for B_d and B_s mixing in the SM, respectively, thus pushing the uncertainty of simulations with 2+1 dynamical flavours below the 10% benchmark for the first time. The FNAL/MILC results dominate the current FLAG average [13] and we get the following predictions[1]

$$\Delta M_d^{\text{FLAG 2019}} = \left(0.582^{+0.049}_{-0.056}\right)\text{ps}^{-1} = \left(1.15^{+0.10}_{-0.11}\right)\Delta M_d^{\text{exp}}\,, \tag{1.5}$$

$$\Delta M_s^{\text{FLAG 2019}} = \left(20.1^{+1.2}_{-1.6}\right)\text{ps}^{-1} = \left(1.13^{+0.07}_{-0.09}\right)\Delta M_s^{\text{exp}}\,, \tag{1.6}$$

which, when combined, are about two standard deviations above the experimental numbers. The values in eq. (1.5) and eq. (1.6) for the mass differences could be the starting point of new anomalies arising in the b-sector, see e.g. [14–18]. In addition ΔM_s poses very severe constraints on certain BSM models — in particular Z' models — that address the observed anomalies in $b \to s\ell\ell$ transitions, see e.g. [19].

To date several new determinations of the matrix elements with a precision below 10% have appeared: first from sum rules [20–24] and very recently from the HPQCD collaboration [25]. The SU(3) breaking ratios were also evaluated by the RBC/UKQCD collaboration [26]. We compare the various predictions in figure 1 where also the results using a weighted average of the values of [13, 23–26] for the matrix elements are shown. The weighted average gives an impressive leap of the precision to 3.6% and 3.1% for the matrix elements for B_d and B_s mixing. We observe excellent agreement between the sum rule prediction and the weighted average and given that lattice simulations and sum rules have very different systematic uncertainties this is a strong confirmation of both methods. We discuss the status of the non-perturbative input in more detail in section 2. With respect to eq. (1.5) and eq. (1.6) the weighted averages

$$\Delta M_d^{\text{Average 2019}} = \left(0.533^{+0.022}_{-0.036}\right)\text{ps}^{-1} = \left(1.05^{+0.04}_{-0.07}\right)\Delta M_d^{\text{exp}}\,, \tag{1.7}$$

$$\Delta M_s^{\text{Average 2019}} = \left(18.4^{+0.7}_{-1.2}\right)\text{ps}^{-1} = \left(1.04^{+0.04}_{-0.07}\right)\Delta M_s^{\text{exp}}\,, \tag{1.8}$$

show better agreement with experiment and a reduction of the total errors by about 40% to the point where the hadronic and parametric CKM uncertainties are of the same size.

We study the mass difference within the SM in more detail in section 2 and give our estimate for the accuracy of the matrix elements in about five years time. Together with

[1] In [12] FNAL/MILC quote as predictions $\Delta M_d^{\text{FNAL/MILC 2016}} = (0.630 \pm 0.069)\,\text{ps}^{-1}$ and $\Delta M_s^{\text{FNAL/MILC 2016}} = (19.6 \pm 1.6)\,\text{ps}^{-1}$. The small difference with respect to our quoted values stems from a different treatment of CKM inputs.

JHEP12(2019)009

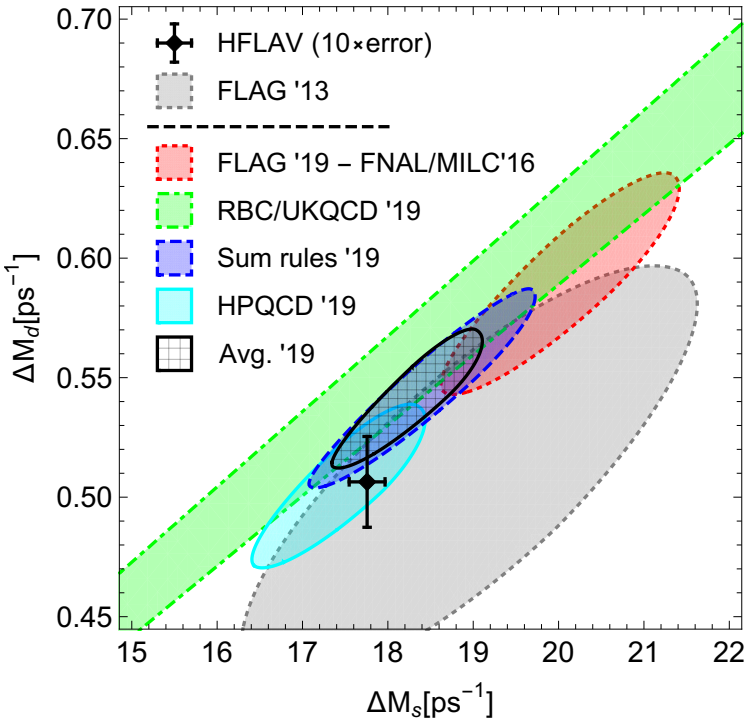

Figure 1. Predictions for ΔM_s and ΔM_d. See section 2 for details.

the extrapolation for the precision of the CKM elements presented in [27] we expect

$$\Delta M_s^{\text{Future 2025}} = (18.4 \pm 0.5)\,\text{ps}^{-1} = (1.04 \pm 0.03)\,\Delta M_s^{\text{exp}}\,, \tag{1.9}$$

for a future ($\sim$ 2025) scenario when the current $b \to s\ell\ell$ anomalies should be established at the level of about 10 standard deviations if the central values remain the same [28]. In section 3 we investigate the implications of B_s mixing on the $b \to s\ell\ell$ anomalies in the FLAG '19, Average '19 and Future '25 scenarios. First, we assume minimal Z' and lepto-quark (LQ) scenarios with only the couplings required to address the anomalies. Then, we discuss the viability of model-building ideas beyond the minimal Z' scenario that might reduce the theory value for ΔM_s and thus improve the agreement with experiment. Finally, we conclude in section 4.

2 ΔM_s in the Standard Model

In the SM, B_s mixing is generated by the diagrams shown in figure 2. The observable of interest in this work is the mass difference of the two mass eigenstates:

$$\Delta M_s \equiv M_H^s - M_L^s = 2\,|M_{12}^s|\,. \tag{2.1}$$

The SM calculation (see e.g. [1] for a review) gives the following result for M_{12}^s

$$M_{12}^{s,\text{SM}} = \frac{G_F^2}{12\pi^2}\lambda_t^2 M_W^2 S_0(x_t)\hat{\eta}_B f_{B_s}^2 M_{B_s} B_1\,, \tag{2.2}$$

JHEP12(2019)009

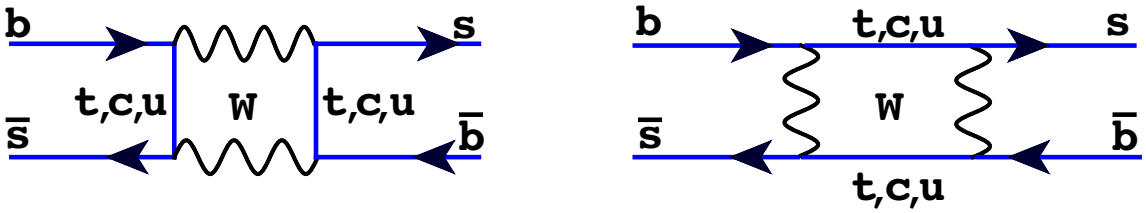

Figure 2. Box diagrams that generate the B_s-$\overline{B}_s$ mixing process in the SM. M_{12}^s is generated when the internal particles are off-shell.

where $\lambda_t = V_{tb}V_{ts}^*$, S_0 is the Inami-Lim function [29], $x_t = (\bar{m}_t(\bar{m}_t)/M_W)^2$ and $\hat{\eta}_B \approx 0.84$ encodes the 2-loop perturbative QCD corrections [30]. In the SM, only a single four-quark $\Delta B = 2$ operator arises,

$$Q_1 = \bar{s}\gamma^\mu(1-\gamma^5)b\ \bar{s}\gamma_\mu(1-\gamma^5)b\,, \tag{2.3}$$

whose hadronic matrix element is parameterised in terms of the meson decay constant f_{B_s} and a bag parameter B_1

$$\langle Q_1\rangle = \langle B_s|Q_1|\overline{B}_s\rangle \equiv \frac{8}{3}M_{B_s}^2 f_{B_s}^2 B_1(\mu_b)\,. \tag{2.4}$$

Note that we have used a form of eq. (2.2) (matching that in [1]) where the bag parameter B_1 depends on the b quark scale $\mu_b \sim m_b$. An alternative notation (commonly used by lattice groups, for example see FLAG [13]) uses the pair $(\eta_B, \hat{B}_1)$ instead of $(\hat{\eta}_B, B_1(\mu_b))$, with $\hat{B}_1$ a renormalization group (RG) invariant quantity. The two are related such that their product is equal, and explicitly we have

$$\hat{B}_1 = \alpha_s(\mu_b)^{-6/23}\left(1+\frac{\alpha_s(\mu_b)}{4\pi}\frac{5165}{3174}\right)B_1(\mu_b) = 1.519\,B_1(\mu_b)\,. \tag{2.5}$$

The combination $f_{B_s}^2 B_1$ is the least-well known parameter for B_s mixing, and the most important as the observable ΔM_s is directly proportional to it. In the SM determination of the decay rate difference $\Delta\Gamma_q$ and for BSM contributions to ΔM_q in addition to Q_1 four more operators arise:

$$\begin{aligned} Q_2 &= \bar{s}_i(1-\gamma^5)b_i\ \bar{s}_j(1-\gamma^5)b_j\,, & Q_3 &= \bar{s}_i(1-\gamma^5)b_j\ \bar{s}_j(1-\gamma^5)b_i\,, \\ Q_4 &= \bar{s}_i(1-\gamma^5)b_i\ \bar{s}_j(1+\gamma^5)b_j\,, & Q_5 &= \bar{s}_i(1-\gamma^5)b_j\ \bar{s}_j(1+\gamma^5)b_i\,, \end{aligned} \tag{2.6}$$

which are typically parameterised as

$$\begin{aligned} \langle Q_2\rangle &= f_{B_s}^2 M_{B_s}^2 \frac{-5M_{B_s}^2}{3(\bar{m}_b(\mu_b)+\bar{m}_s(\mu_b))^2}B_2(\mu_b)\,, \\ \langle Q_3\rangle &= f_{B_s}^2 M_{B_s}^2 \frac{M_{B_s}^2}{3(\bar{m}_b(\mu_b)+\bar{m}_s(\mu_b))^2}B_3(\mu_b)\,, \\ \langle Q_4\rangle &= f_{B_s}^2 M_{B_s}^2 \left[\frac{2M_{B_s}^2}{(\bar{m}_b(\mu_b)+\bar{m}_s(\mu_b))^2}+\frac{1}{3}\right]B_4(\mu_b)\,, \\ \langle Q_5\rangle &= f_{B_s}^2 M_{B_s}^2 \left[\frac{2M_{B_s}^2}{3(\bar{m}_b(\mu_b)+\bar{m}_s(\mu_b))^2}+1\right]B_5(\mu_b)\,. \end{aligned} \tag{2.7}$$

JHEP12(2019)009

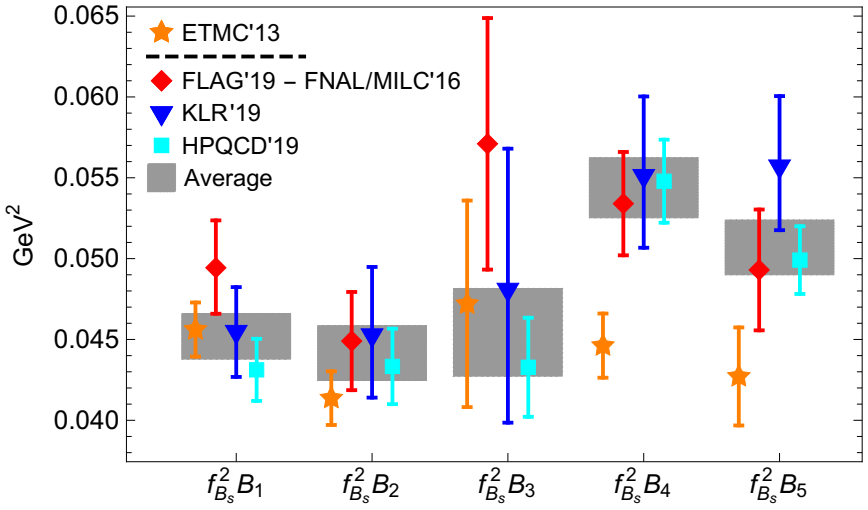

Figure 3. Comparison of non-perturbative determinations of the matrix elements for B_s mixing at the scale $\mu_b = \bar{m}_b(\bar{m}_b)$. We show the ETMC '13 values in orange, the FLAG 2+1 average [13] for the operator Q_1 together with the FNAL/MILC '16 results [12] for the other operators in red, the sum rule values [24] in blue and the HPQCD '19 results [25] in cyan. The gray rectangles indicate the weighted averages of the first three determinations.

The full basis of matrix elements has been determined with lattice simulations [12, 25, 31] and sum rules [23, 24]. In [12] the combinations $f_{B_s}^2 B_i$ were determined and combined with the 2016 PDG average for the decay constants to extract the Bag parameters. This implies that the latter suffer from bigger uncertainties because one cannot exploit partial cancellations of uncertainties which occur when f_{B_s} is determined in the same simulation. All other works determine the Bag parameters $B_i(\mu_b)$ as their central results. This has the advantage that the values can easily be combined with updated results for the decay constant f_{B_s} which has seen significant improvements in the last few years and we use the FLAG 2+1+1 average [13] of the results [32–34] below.

In fact the sum rule method directly determines the Bag parameters and requires an independent result for the decay constant to obtain the matrix elements. In this approach one has to determine the perturbative 3-loop contribution to a correlator describing B mixing. Based on the master integrals presented in [35] this calculation was first performed for B_d mixing by [20–22] and confirmed in [23], where this method was also extended to different mixing operators and to lifetime operators. In [24] corrections due to a finite value of the strange quark mass were determined, yielding new predictions for the mass differences in better agreement with experiment than the FNAL/MILC values (eqs. (1.5) and (1.6)) with similar precision.

Very recently an independent lattice study was performed by HPQCD [25] which does not confirm the large FNAL/MILC predictions for the mass differences. We present a comparison of the combinations $f_{B_s}^2 B_i$ in figure 3. Besides the individual results [12, 13, 24, 25, 31] we show the weighted averages thereof where we have excluded [31] which only uses two dynamical flavours. For $f_{B_s}^2 B_1$, which determines the SM value of the mass difference,

JHEP12(2019)009

the FLAG '19 and HPQCD '19 values do not overlap. However, the overall average shows perfect agreement with the KLR '19 and ETMC '13 results despite the very different systematic uncertainties of lattice simulation and sum rules. This makes us confident that the weighted average represents a reliable assessment of the current uncertainties. The different values of $f_{B_s}^2 B_2$ agree well. The case of $f_{B_s}^2 B_3$ is similar to that of the SM matrix element but the uncertainties are considerably larger. Finally for $f_{B_s}^2 B_4$ and $f_{B_s}^2 B_5$ we find a discrepancy between the results from ETMC '13 and the remaining ones. This difference might result from the use of RI-MOM renormalisation scheme in [31], see e.g. the discussion in [36] for a similar problem in the K sector. The other values are in good agreement with each other, with KLR '19 yielding a somewhat larger result than the lattice simulations for $f_{B_s}^2 B_5$. Our weighted averages at the scale $\mu_b = \bar{m}_b(\bar{m}_b)$ read

$$\begin{aligned}
f_{B_s}^2 B_1(\mu_b) &= (0.0452 \pm 0.0014)\,\text{GeV}^2\,,\\
f_{B_s}^2 B_2(\mu_b) &= (0.0441 \pm 0.0017)\,\text{GeV}^2\,,\\
f_{B_s}^2 B_3(\mu_b) &= (0.0454 \pm 0.0027)\,\text{GeV}^2\,,\\
f_{B_s}^2 B_4(\mu_b) &= (0.0544 \pm 0.0019)\,\text{GeV}^2\,,\\
f_{B_s}^2 B_5(\mu_b) &= (0.0507 \pm 0.0017)\,\text{GeV}^2\,.
\end{aligned} \tag{2.8}$$

For convenience we also provide the weighted averages for B_d mixing and the Bag parameters in A.

The ratio of the mass differences of B_s and B_d mesons benefits from the cancellation of many uncertainties and in the SM we get

$$\frac{\Delta M_d}{\Delta M_s} = \left|\frac{V_{td}^2}{V_{ts}^2}\right| \frac{M_{B_d}}{M_{B_s}} \frac{f_B^2 B_1^{B_d}}{f_{B_s}^2 B_1^{B_s}} \equiv \left|\frac{V_{td}^2}{V_{ts}^2}\right| \frac{M_{B_d}}{M_{B_s}} \xi^{-2}\,. \tag{2.9}$$

Different determinations [12, 13, 21, 24–26, 31] of the ratio ξ are compared in figure 4 and we observe good agreement. The weighted average

$$\xi = 1.200^{+0.0054}_{-0.0060} \tag{2.10}$$

of the values from [13, 24–26] is dominated by the sum rule result [24] which is about a factor of two more precise than the lattice determinations. Using the CKMFitter result

$$|V_{td}/V_{ts}| = 0.2088^{+0.0016}_{-0.0030}\,, \tag{2.11}$$

the ratio of the mass differences becomes

$$\left(\frac{\Delta M_d}{\Delta M_s}\right)_{\text{exp}} = 0.0285 \pm 0.0001\,, \tag{2.12}$$

$$\left(\frac{\Delta M_d}{\Delta M_s}\right)_{\text{Average}} = 0.0298^{+0.0005}_{-0.0009} = 0.0297^{+0.0003}_{-0.0003}\,(\text{had.})^{+0.0005}_{-0.0008}\,(\text{CKM})\,, \tag{2.13}$$

where the parametric CKM uncertainty (2.11) dominates theory error. We note that there is a slightly discrepancy between our average and experiment, at the level of $\sim 1.4\,\sigma$.

JHEP12(2019)009

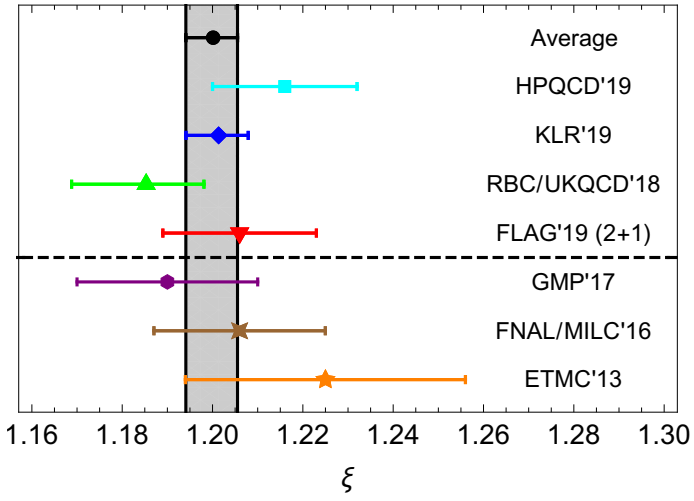

Figure 4. Comparison of determinations of the SU(3)-flavour breaking ratio ξ. The gray band corresponds to the weighted average of the results [13, 24–26]. Below the dashed line we also show the values from [12, 21, 31] which are not included in the average.

This allows a very precise determination of $|V_{td}/V_{ts}|$ from B mixing [24]. We note that the product of (2.13) and (1.8) is about 3% larger than the value for ΔM_d from a direct determination (1.7). The reason is that we also include the RBC/UKQCD '18 [26] result in the average (2.10) for ξ but not in the averages for the individual matrix elements since those were not determined there.[2] The ellipses in figure 1 use $f_{B_s}^2 B_1$ and ξ as inputs and the ellipse for the weighted average therefore also gives a value of ΔM_d which is about 3% larger than (1.7). We further note that our ellipses for the FLAG '19 and HPQCD '19 results differ from the numerical results given in [12] and [25] because we use different values for the CKM parameters as discussed in A.

All in all we observe a consistent picture of different non-perturbative determinations for B mixing. The future ($\sim$ 2025) prospects for lattice simulations of the matrix elements have been assessed in [27, 37]. The relative uncertainties for $f_{B_s}^2 B_1$ are estimated as 3% [27] and 1.3% [37]. Given that the two latest lattice results [12, 25] do not overlap within their uncertainties and differ by 15% we believe the latter estimate to be overly optimistic and assume the scenario of [27]. On the other hand the uncertainties in sum rule analyses are dominated by the one from the matching between QCD and Heavy Quark Effective Theory (HQET) matrix elements which can be reduced significantly by a perturbative two-loop matching calculation [21, 22] or eliminated altogether by using QCD [38, 39] instead of HQET sum rules. We expect that a reduction of the sum rule uncertainty for B_1 to 3% is realistic. The effect on the weighted average is a reduction of the error from 3.1% to about 2%.

Simultaneously, new experimental data from Belle II and the LHC will improve our knowledge of the CKM element V_{cb} which constrains V_{ts} in the CKM unitarity fits and is the other critical input to our theory predictions. The Belle II collaboration forecasts [27] that by 2025 the uncertainty on V_{cb} will be at the level of 1%. Using these future predictions

[2] Furthermore the mean of a ratio is not the same as the ratio of the means.

JHEP12(2019)009

Parameter	Future value
V_{cb}	$0.04240 \pm 1\% = 0.04240 \pm 0.00042$
$f_{B_s}\sqrt{\hat{B}_1}$	$(262 \pm 1\%)\,\text{MeV} = (262.0 \pm 2.6)\,\text{MeV}$

Table 1. Future values for the two most important parameters for the error on ΔM_s.

(our explicit future inputs are given in table 1, with all others staying the same as at present), we expect that ΔM_s will be predicted with an uncertainty of only $\pm 0.5\,\text{ps}^{-1}$ by 2025, yielding eq. (1.9).[3]

3 ΔM_s interplay with flavour anomalies

3.1 Status and future prospects of the $b \to s\ell\ell$ anomalies

A key application of the refined SM prediction for ΔM_s is in the context of the recent hints of lepton flavour universality (LFU) violation in semi-leptonic B meson decays. Focussing on neutral current anomalies, the main observables are the LFU violating ratios $R_{K^{(*)}} \equiv \mathcal{B}(B \to K^{(*)}\mu^+\mu^-)/\mathcal{B}(B \to K^{(*)}e^+e^-)$ [40–42], together with the angular distributions of $B \to K^{(*)}\mu^+\mu^-$ [43–52] and the branching ratios of hadronic $b \to s\mu^+\mu^-$ decays [43, 44, 53]. The effective Lagrangian for semi-leptonic $b \to s\mu^+\mu^-$ transitions contains the terms

$$\mathcal{L}^{\text{NP}}_{b\to s\mu\mu} \supset \frac{4G_F}{\sqrt{2}} V_{tb}V_{ts}^* \left(\delta C_9^\mu O_9^\mu + \delta C_{10}^\mu O_{10}^\mu + \delta C_9^{\prime\mu} O_9^{\prime\mu} + \delta C_{10}^{\prime\mu} O_{10}^{\prime\mu}\right) + \text{h.c.}\,, \tag{3.1}$$

with

$$O_9^\mu = \frac{\alpha}{4\pi}(\bar{s}_L\gamma_\mu b_L)(\bar{\mu}\gamma^\mu\mu)\,, \tag{3.2}$$

$$O_{10}^\mu = \frac{\alpha}{4\pi}(\bar{s}_L\gamma_\mu b_L)(\bar{\mu}\gamma^\mu\gamma_5\mu)\,, \tag{3.3}$$

and the primed operators $O^{\prime\mu}_{9,10}$ having the opposite ($L \to R$) quark chiralities. Intriguingly, one obtains a very good description of the $b \to s\ell\ell$ data by allowing new physics only in a single combination of Wilson coefficients (for recent fits see e.g. [54–60]). The best-fit scenario $\delta C_9^\mu = -\delta C_{10}^\mu \approx -0.53 \pm 0.08$ of [54] corresponds to an effective operator with left-handed (LH) quark and muon currents and we consider its interplay with ΔM_s in section 3.4. The data is also well represented by assuming either δC_9^μ or δC_{10}^μ being different from zero, corresponding to vector or axial-vector muon currents, respectively. However, we find that the mixing constraints on these scenarios are stronger than for case of LH muon currents, since larger values of the Wilson coefficients are required, and do not discuss them further. Following the update of R_K from LHCb [42], there has been an increased favourability of right handed (RH) current contributions in the quark sector and we investigate their effect in section 3.5.2.

[3] It is worth noting that with such a precision, the FLAG 2019 central value given in eq. (1.6) is almost $5\,\sigma$ away from the experimental result.

JHEP12(2019)009

By 2025 LHCb expects a serious improvement in the measured precision on R_K and R_{K^*} compared to the situation today — they forecast [28] the error on R_K will be reduced to ± 0.025 (better than a factor of two compared to the error reported at Moriond 2019) and to ± 0.031 for R_{K^*} (a factor of four better). If these precisions are indeed realised, and the central values stay close to their currently measured values, LHCb will have made a discovery of LFU violation at the level of $6\,\sigma$ and $10\,\sigma$ for R_K and $R_{K^{(*)}}$ respectively.

3.2 New physics contributions to ΔM_s in the effective theory

The NP contributions to B_s mixing can be described by the effective Lagrangian

$$\mathcal{L}^{\rm NP}_{\Delta B=2} \supset -\frac{4G_F}{\sqrt{2}}\left(V_{tb}V_{ts}^*\right)^2\Big[C_{bs}^{LL}\left(\bar{s}_L\gamma_\mu b_L\right)^2 + C_{bs}^{RR}\left(\bar{s}_R\gamma_\mu b_R\right)^2 + C_{bs}^{LR}\left(\bar{s}_L\gamma_\mu b_L\right)\left(\bar{s}_R\gamma^\mu b_R\right)\Big] + \text{h.c.}\,, \tag{3.4}$$

where we assume NP only gives rise to vector colour singlet operators. The full basis of $\Delta B = 2$ operators (eqs. (2.3) and (2.6)) also contains operators that give tensor or scalar Dirac structures when written in colour singlet form. However, these operator structures are highly disfavoured by the fits to $b \to s\ell\ell$ data, and so we ignore them here. Assuming the NP coefficients C_{bs} are generated at some higher scale $\mu_{\rm NP}$, we have to include RG running effects down to the b quark scale (see e.g. [61]), which brings in the LR vector operator with the non colour singlet structure through operator mixing and explains the appearance of both B_4 and B_5 in the expression below. In this way we can parameterise the SM+NP contribution normalized to the SM one as[4]

$$\frac{\Delta M_s^{\rm SM+NP}}{\Delta M_s^{\rm SM}} = \left|1 + \frac{\eta^{6/23}}{R^{\rm SM}_{\rm loop}}\left\{C_{bs}^{LL} + C_{bs}^{RR} - \frac{C_{bs}^{LR}}{2\eta^{3/23}}\left[\frac{B_5}{B_1}\left(\frac{M_{B_s}^2}{(m_b+m_s)^2}+\frac{3}{2}\right) + \frac{B_4}{B_1}\left(\frac{M_{B_s}^2}{(m_b+m_s)^2}+\frac{1}{6}\right)\left(\eta^{-27/23}-1\right)\right]\right\}\right|, \tag{3.5}$$

with $\eta = \alpha_s(\mu_{\rm NP})/\alpha_s(m_b)$, the bag parameters B_i defined as in eqs. (2.4) and (2.7), and the SM loop function given by

$$R^{\rm loop}_{\rm SM} = \frac{\sqrt{2}G_F M_W^2 \hat{\eta}_B S_0(x_t)}{16\pi^2} = (1.310 \pm 0.010)\times 10^{-3}\,. \tag{3.6}$$

In general, one would expect that any NP contributing to $b \to s\ell\ell$ transitions will eventually feed into B_s mixing. However, this connection is hidden at the effective operator level where the Wilson coefficients in eq. (3.1) and eq. (3.5) are independent.[5] It is hence crucial to focus on specific UV realizations in order to explore the connection between $b \to s\ell\ell$ anomalies and ΔM_s and we will consider two simplified models below.

[4] This expression neglects the top-quark threshold, which is a sub-percent effect. However, the correct running is taken into account in our numerics and figures.

[5] The double insertion of the effective Lagrangian for $b \to s\ell\ell$ transitions (3.1) yields a contribution to ΔM_s at the dimension-eight level. Compared to the contribution from eq. (3.5) this is suppressed by $m_b^2/\Lambda_{\rm NP}^2$ and cannot be used to obtain meaningful constraints.

JHEP12(2019)009

3.3 Simplified models for the $b \to s\ell\ell$ anomalies

There are two basic possibilities how the effective operators in eq. (3.1) can be generated at tree level: by the exchange of a Z' mediator coupling to the quark and the muon current or by the exchange of a lepto-quark coupling to mixed quark-muon currents. Anticipating our results from section 3.4 we describe the Z' scenario in detail below. In addition we consider the case of the scalar lepto-quark $S_3 \sim (3, 3, 1/3)$, whose defining Lagrangian can be found e.g. in [19, 62].

We consider a simplified Z' model with only those couplings required to explain the observed flavour anomalies, with the Lagrangian

$$\mathcal{L}_{Z'} \supset \frac{1}{2} M_{Z'}^2 (Z'_\mu)^2 + Z'_\mu \left(\lambda^Q_{ij} \bar{d}^i_L \gamma^\mu d^i_L + \lambda^d_{ij} \bar{d}^i_R \gamma^\mu d^j_R + \lambda^L_{ij} \bar{\ell}^i_L \gamma^\mu \ell^j_L \right) , \tag{3.7}$$

where d^i and ℓ^i label the different generations of down-type quark and charged lepton mass eigenstates respectively, and $\lambda^{Q,d,L}$ are hermitian flavour space matrices. We have neglected RH currents in the lepton sector in the above eq. (3.7) since the latter actually worsen the compatibility with ΔM_s, as they require a larger Wilson coefficient.

Integrating out the Z' at tree level, we get the effective Lagrangian

$$\begin{aligned} \mathcal{L}^{\text{eff}}_{Z'} \supset -\frac{1}{2M_{Z'}^2} \Big(& 2\lambda^Q_{23}\lambda^L_{22} (\bar{s}_L \gamma^\mu b_L)(\bar{\mu}_L \gamma_\mu \mu_L) + 2\lambda^d_{23}\lambda^L_{22} (\bar{s}_R \gamma^\mu b_R)(\bar{\mu}_L \gamma_\mu \mu_L) \\ & + \left(\lambda^Q_{23}\right)^2 (\bar{s}_L \gamma^\mu b_L)(\bar{s}_L \gamma_\mu b_L) \\ & + \left(\lambda^d_{23}\right)^2 (\bar{s}_R \gamma^\mu b_R)(\bar{s}_R \gamma_\mu b_R) + 2\lambda^Q_{23}\lambda^d_{23} (\bar{s}_L \gamma^\mu b_L)(\bar{s}_R \gamma_\mu b_R) \Big) . \end{aligned} \tag{3.8}$$

The first line contains the terms that contribute to the rare decay coefficients $C^{(\prime)\mu}_{9,10}$, the second a contribution to ΔM_s through the same operator as in the SM, and the third contributions to ΔM_s from operators that do not appear in the SM.

Matching onto the effective Lagrangians for the low energy observables in eqs. (3.1) and (3.4), we find (at the scale $\mu = M_{Z'}$)

$$\delta C^\mu_9 = -\delta C^\mu_{10} = -\frac{\pi}{\sqrt{2} G_F M_{Z'}^2 \alpha} \left(\frac{\lambda^Q_{23}\lambda^L_{22}}{V_{tb}V^*_{ts}} \right) , \tag{3.9}$$

$$\delta C'^\mu_9 = -\delta C'^\mu_{10} = -\frac{\pi}{\sqrt{2} G_F M_{Z'}^2 \alpha} \left(\frac{\lambda^d_{23}\lambda^L_{22}}{V_{tb}V^*_{ts}} \right) , \tag{3.10}$$

$$C^{LL}_{bs} = \frac{1}{4\sqrt{2} G_F M_{Z'}^2} \left(\frac{\lambda^Q_{23}}{V_{tb}V^*_{ts}} \right)^2 , \tag{3.11}$$

$$C^{RR}_{bs} = \frac{1}{4\sqrt{2} G_F M_{Z'}^2} \left(\frac{\lambda^d_{23}}{V_{tb}V^*_{ts}} \right)^2 , \tag{3.12}$$

$$C^{LR}_{bs} = \frac{\sqrt{2}}{4 G_F M_{Z'}^2} \left(\frac{\lambda^Q_{23}\lambda^d_{23}}{(V_{tb}V^*_{ts})^2} \right) . \tag{3.13}$$

JHEP12(2019)009

Inserting the above expressions in eq. (3.5), using our combined averages for the bag parameters, and taking a typical Z' scale of 5 TeV we find that the contribution to ΔM_s can be written as[6]

$$\frac{\Delta M_s^{\rm SM+NP}}{\Delta M_s^{\rm SM}} \approx \left| 1 + 200 \left(\frac{5\,\text{TeV}}{M_{Z'}}\right)^2 \left[\left(\lambda^Q_{23}\right)^2 + \left(\lambda^d_{23}\right)^2 - 9\lambda^Q_{23}\lambda^d_{23} \right] \right| , \tag{3.14}$$

which shows a significant RG enhancement for the LR operator.

Besides B_s mixing, we consider a constraint that is particularly relevant for light Z' interacting with muons via LH currents. By $\mathrm{SU}(2)_L$ invariance the Z' couples also to LH neutrinos via the λ^L_{22} coupling which is required by the $b \to s\mu\mu$ anomalies. Hence, one has an extra term in the Z' effective Lagrangian of the type

$$\mathcal{L}^{\rm eff}_{Z'} \supset -\frac{(\lambda^L_{22})^2}{M^2_{Z'}} (\bar{\mu}_L \gamma^\mu \mu_L)(\bar{\nu}_{\mu L} \gamma^\mu \nu_{\mu L}) \,, \tag{3.15}$$

which leads to the neutrino trident production, $\nu_\mu N \to \nu_\mu \mu^+ \mu^- N$. Using the most recent calculation for the SM cross-section, one gets [63]

$$\frac{\sigma^{\rm SM+NP}_{\rm CCFR}}{\sigma^{\rm SM}_{\rm CCFR}} = \frac{1.13 \left(1 + \frac{v^2 (\lambda^L_{22})^2}{M^2_{Z'}}\right)^2 + \left(1 + 4 s^2_W + \frac{v^2 (\lambda^L_{22})^2}{M^2_{Z'}}\right)^2}{1.13 + (1 + 4 s^2_W)^2} \tag{3.16}$$

(with $v \approx 246\,\text{GeV}$ and $s^2_W \approx 0.231$), which is constrained by the existing CCFR measurement $\sigma_{\rm CCFR}/\sigma^{\rm SM}_{\rm CCFR} = 0.82 \pm 0.28$ [64]. This result implies $M_{Z'}/\lambda^L_{22} > 0.47\,\text{TeV}$ at $2\,\sigma$. The upcoming DUNE experiment [65] is expected to also measure this process, however the precision it will achieve (see e.g. [63]), suggest its data will not increase much the limits on this parameter combination and so we will use the CCFR bound throughout.

Last but not least, the parameter space is constrained by direct LHC searches [66, 67] and perturbative unitarity [68, 69]. Whether a few TeV Z' is ruled out by LHC direct searches crucially depends on the details of the Z' model. The stringent constraints from di-lepton searches [66] are tamed in models where the Z' does not couple to valence quarks. For instance, assuming only the two couplings required by the $b \to s\ell\ell$ anomaly, namely λ^Q_{23} and λ^L_{22}, one finds that current Z' searches are not sensitive yet (see e.g. [70, 71]). Assuming the best-fit scenario $\delta C^\mu_9 = -\delta C^\mu_{10} \approx -0.53 \pm 0.08$ [54] is generated by the exchange of a Z' we obtain the perturbative unitarity bound $M_{Z'} < 59\,\text{TeV}$ [68]. The same limit for the lepto-quark scenario reads $M_{S_3} < 69\,\text{TeV}$ [68]. The mass of the lepto-quark is also bounded from below up to about 1 TeV [67] from direct searches at the LHC.

3.4 ΔM_s interplay with flavour anomalies in the minimal scenarios

We investigate which new physics contributions $\Delta M^{\rm NP}_s$ to the B_s mass difference are generated by the simplified models of section 3.3, assuming LH currents in the quark sector

[6] The prefactor and the relative size of the interference term have a sub-leading logarithmic dependence from the Z' mass (less than 1% for $M_{Z'}$ in the 1–10 TeV range).

JHEP12(2019)009

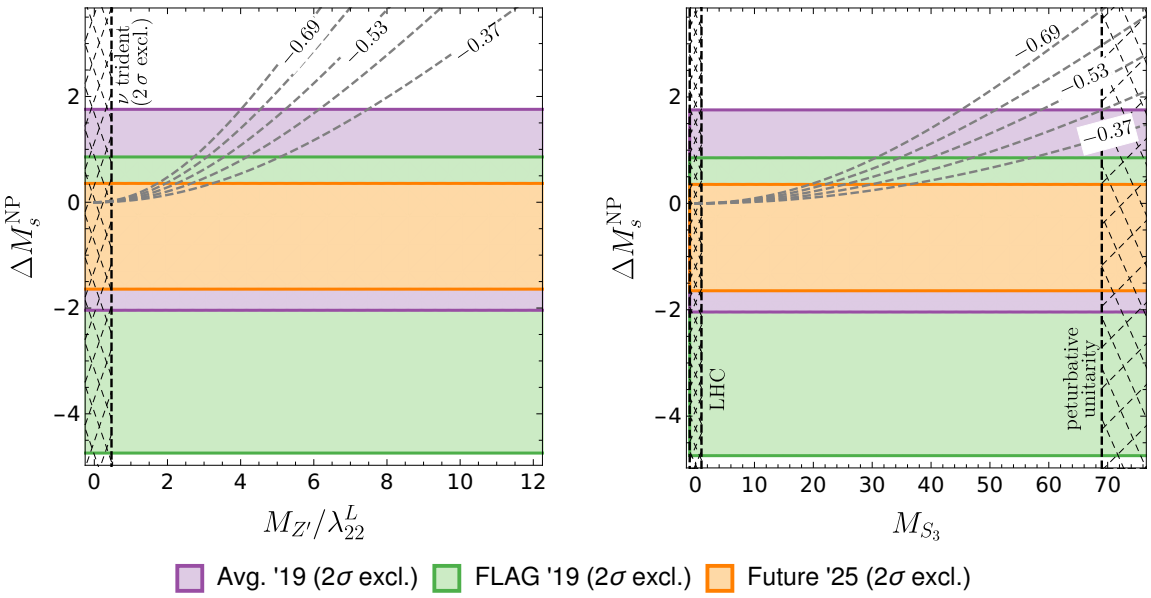

Figure 5. We show the predicted new physics effects $\Delta M_s^{\rm NP}$ (dashed lines) for various values of $\delta C_9^\mu = -\delta C_{10}^\mu$ in comparison with the allowed two-sigma regions (shaded) in the FLAG '19, Avg. '19 and Future '25 scenarios. The left and right panel assume the simplified Z' model and scalar lepto-quark model, respectively. Hatched regions show limits from neutrino trident production or direct LHC searches and perturbative unitarity.

and real couplings (these two assumptions will be relaxed in section 3.5). We obtain the predictions

$$\begin{aligned}\frac{\Delta M_s^{\rm SM+NP}}{\Delta M_s^{\rm SM}} &= \left|1 + \frac{G_F \alpha_{\rm EM}^2 \eta^{6/23}}{2\sqrt{2}\pi^2 R_{\rm loop}^{\rm SM}} \left(\delta C_9^\mu = -\delta C_{10}^\mu\right)^2 \left(\frac{M_{Z'}}{\lambda_{22}^L}\right)^2\right| \\ &\approx \left|1 + \frac{1}{360}\left(\frac{\delta C_9^\mu = -\delta C_{10}^\mu}{-0.53}\right)^2 \left(\frac{M_{Z'}/\lambda_{22}^L}{1\,\text{TeV}}\right)^2\right|,\end{aligned} \tag{3.17}$$

for the Z' and

$$\begin{aligned}\frac{\Delta M_s^{\rm SM+NP}}{\Delta M_s^{\rm SM}} &= \left|1 + \frac{G_F \alpha_{\rm EM}^2 \eta^{6/23}}{2\sqrt{2}\pi^2 R_{\rm loop}^{\rm SM}} \frac{5}{64\pi^2} \left(\delta C_9^\mu = -\delta C_{10}^\mu\right)^2 \left(M_{S_3}\right)^2\right| \\ &\approx \left|1 + \frac{1}{29\,000}\left(\frac{\delta C_9^\mu = -\delta C_{10}^\mu}{-0.53}\right)^2 \left(\frac{M_{S_3}}{1\,\text{TeV}}\right)^2\right|,\end{aligned} \tag{3.18}$$

for the lepto-quark.

In figure 5 we compare the new physics contributions $\Delta M_s^{\rm NP}$ in the two models to the allowed two-sigma regions for the present and future scenarios. The dashed lines show what effect is predicted for a given value of the Wilson coefficient combination $\delta C_9^\mu = -\delta C_{10}^\mu$, whereby the envelope of these lines corresponds to the two-sigma region from the fit

JHEP12(2019)009

$\delta C_9^\mu = -\delta C_{10}^\mu = -0.53 \pm 0.08$ to the present $b \to s\ell\ell$ data. In addition we show constraints from neutrino trident production, direct searches by the LHC experiments and perturbative unitarity as hatched regions.

The left plot shows the simplified Z' model where the relation between ΔM_s and δC_9 depends on the parameter combination $M_{Z'}/\lambda_{22}^L$. We observe that a Z' explanation of the $b \to s\ell\ell$ data causes a sizeable positive contribution to ΔM_s unless the Z' mass is rather light. Values of $\Delta M_s^{\rm NP}$ outside the shaded regions are in tension with the respective predictions for ΔM_s at the level of two standard deviations. This allows us to place upper bounds on the mass of the Z'.[7] For instance, we find that the large central value of the FLAG '19 prediction in eq. (1.6) (green region) requires $M_Z'/\lesssim 4\,\text{TeV}$ for $\lambda_{22}^L = 1$ in order to explain $b \to s\ell\ell$ at $1\,\sigma$. The limit is about a factor $3/2$ weaker in the case of the Average '19 value of ΔM_s (purple region) despite the reduction of the uncertainty by over 30% with respect to FLAG '19 because the central value is closer to the experimental result. It is straightforward to rescale the bound for different lepton couplings. The combination of ΔM_s and perturbative unitarity (requiring $\lambda_{22}^L < \sqrt{4\pi}$ The lepto-quark model is shown in the right plot and yields smaller new physics contributions to ΔM_s because the effect is only generated at loop level. Using the Average '19 value (purple) we find that a lepto-quark explanation is still viable in the entire mass range between implies an upper limit of about 30 TeV on the lepto-quark mass M_{S_3}, better than the perturbativity bound by more than a factor of two.

We conclude that both simplified Z' and lepto-quark models currently provide possible solutions to the $b \to s\ell\ell$ anomalies, with the previous stringent constraints [19] from the FLAG '19 values for ΔM_s being relaxed by the refined SM prediction Average '19. However, with the future increase in the precision of ΔM_s lepto-quark explanations will be favoured over a Z', assuming that the central values remain similar. In section 3.5 we therefore discuss ideas how the implied tension might be reduced by generalizations of the minimal Z' scenario.

3.5 New physics options beyond the minimal Z' scenario

The constraints on the minimal Z' scenario considered above are particularly strong because the latter predicts a *positive* contribution to ΔM_s, while the central values of the current SM predictions are already larger than the experimental result. Therefore, we will explore two simple options for how a negative contribution to ΔM_s could be generated, thus relaxing the tension. Examining eq. (3.14) the two cases present themselves:

1. For only LH quark coupling (i.e. $\lambda^d = 0$), a negative contribution can only be generated if λ_{23}^Q acquires a complex phase.

2. With both LH and RH quark couplings, real couplings alone can give the required sign if the interference term is large enough.

[7] A full statistical fit would be in order here to make a definitive statement about some particular model being excluded.

JHEP12(2019)009

Although these two possibilities were already identified in [19], their compatibility with global fits for flavour anomalies was only partially assessed in [72]. We start with CP violating couplings in section 3.5.1, and then study the case for RH quark currents in section 3.5.2. As a benchmark point, we take a lepton coupling of $\lambda^L_{22} = 1$ and a Z' mass of 5 TeV where the best-fit result $\delta C^\mu_9 = -\delta C^\mu_{10} = -0.53$ saturates the two-sigma range of the Average '19 prediction (see figure 5). In the following, we address the question whether either option 1. or 2. allows for this benchmark point to be viable within the FLAG '19 or Future '25 scenarios.

3.5.1 CP violating couplings

It is clear from eq. (3.14) that if λ^Q_{23} has a large enough imaginary part, then it will be possible to bring down the theory prediction for ΔM_s below the SM prediction and into better agreement with experiment. However, once we allow for complex Z' quark couplings, there are extra constraints to be considered, in the form of CP-violating observables that arise from B_s mixing. The most relevant here is the mixing-induced CP asymmetry [1, 73], arising from interference between B meson mixing and decay. The semi-leptonic CP asymmetries for flavour-specific decays, $a^s_{\rm sl}$, are not competitive yet since the experimental errors are still too large [1]. Defining

$$\phi_\Delta = \text{Arg}\left(1 + \frac{\eta^{6/23} C^{LL}_{bs}}{R^{\rm loop}_{\rm SM}}\right), \tag{3.19}$$

(with η as in eq. (3.5)) the mixing-induced CP asymmetry is given by

$$A^{\rm mix}_{\rm CP}(B_s \to J/\psi\phi) = \sin\left(\phi_\Delta - 2\beta_s\right), \tag{3.20}$$

where $A^{\rm mix}_{\rm CP} = -0.021 \pm 0.031$ [2, 74], $\beta_s = 0.01843^{+0.00048}_{-0.00034}$ [75], and we have neglected penguin contributions [1].

New phases in λ^Q_{23} also imply a complex value for δC^μ_9, which has not typically been considered in previous global fits (see [76, 77] for exceptions). We perform our own fit using the `flavio` software [78], using the same set of $b \to s\ell\ell$ observables as [79].

The result of our fit is shown in figure 6, with the higher SM prediction $\Delta M_s^{\text{FLAG '19}}$ corresponding to the green bands. There is no overlap between the $1\,\sigma$ regions for our three observables, since $A^{\rm mix}_{\rm CP}$ provides too strong a constraint on the imaginary part of the coupling. So a complex coupling does not provide a way to significantly evade the strong bounds from ΔM_s. Using instead our prediction $\Delta M_s^{\text{Future '25}}$ (orange) there is still no overlap, for the same reason. As such, the addition of complex phases to the Z' quark coupling does not alleviate tension at the benchmark point in the Future '25 scenario, which is important given the strength of this future bound, as shown in figure 5.

3.5.2 Right-handed couplings

A Z' coupling to a RH quark current can also allow for a negative BSM contribution to ΔM_s through the interference term, which has the advantage that it is RG enhanced by roughly an order of magnitude (see eq. (3.14)) relative to the pure LL or RR operators. In our

JHEP12(2019)009

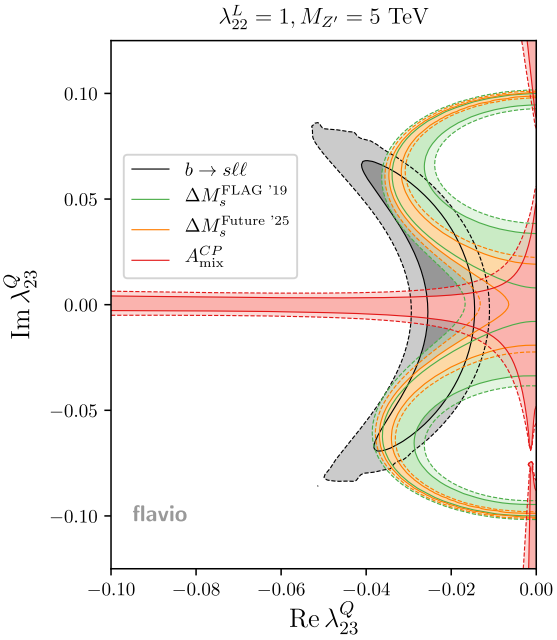

Figure 6. Allowed regions at $1\,\sigma$ (solid) and $2\,\sigma$ (dashed) for $b \to s\ell\ell$ (grey), ΔM_s (green (FLAG '19) and orange (Future '25)), and $A_{\text{mix}}^{\text{CP}}$ (red).

previous work [19, 72] we stated that RH quark currents break the approximate symmetry $R_K \approx R_{K^*}$ and hence were disfavoured by the data. On the other hand, the recent update of R_K at Moriond 2019 [42] favours a non-zero RH quark current contribution, as widely discussed in the literature since then (see e.g. [54–60]).

There is however a problem with this solution, which is that in our Z' model, at the leading order in the NP contribution, the behaviour can be written as

$$\frac{R_K - 1}{R_{K^*} - 1} \approx \frac{\lambda^Q_{23} + \lambda^d_{23}}{\lambda^Q_{23} - (2p-1)\lambda^d_{23}}\,, \tag{3.21}$$

where $p \approx 0.86$ is the polarization fraction [80]. The current experimental measurements suggest $(R_K - 1)/(R_{K^*} - 1) \approx 0.50$, which requires $\lambda^d_{23}/\lambda^Q_{23} \approx -0.37$. On the other hand, eq. (3.14) shows that the same sign for LH and RH quark couplings are needed to reduce ΔM_s. This is evident in our fit result shown in figure 7, where the allowed region for the $b \to s\ell\ell$ anomalies is partially driven by the $R_{K^{(*)}}$ measurements. With the high prediction $\Delta M_s^{\text{FLAG '19}}$, there is a clear gap between the $1\,\sigma$ allowed regions, which does not allow us to solve the tension for the benchmark point (for a similar conclusion see also [58]). If we instead examine the orange region, corresponding to the $\Delta M_s^{\text{Future '25}}$ prediction,[8] the gap has shrunk by only a small amount, and so our benchmark point is only marginally more favoured.

[8]For the numerics here we assume a similar relative improvement in the precision of the BSM bag parameters $B_{4,5}$ as was described earlier for B_1.

JHEP12(2019)009

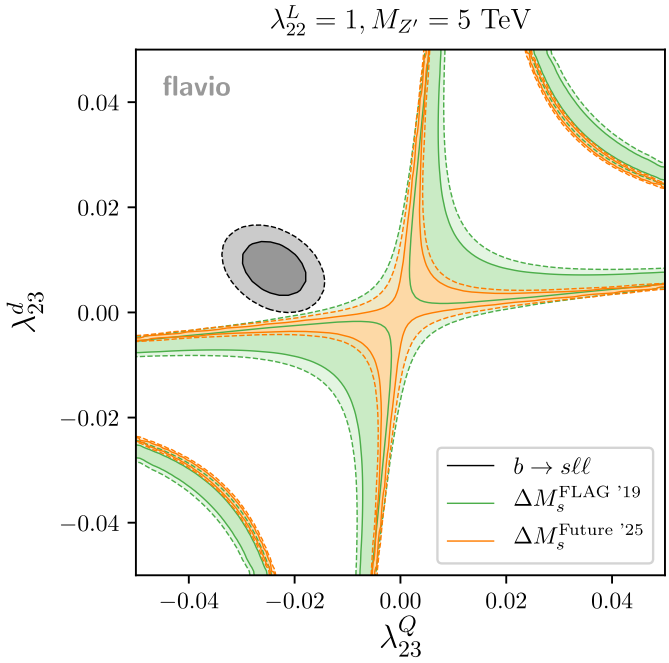

Figure 7. Allowed regions at $1\,\sigma$ (solid) and $2\,\sigma$ (dashed) for $b \to s\ell\ell$ (grey) and ΔM_s (green (FLAG '19) and orange (Future '25)).

3.5.3 Beyond simplified Z' models

Within the simplified Z' model considered so far, neither of the two options above (imaginary couplings and RH quark currents) helps to improve the compatibility between the $b \to s\ell\ell$ measurements and the expected precision determination value of ΔM_s in 2025. There are, however, other possibilities in order to achieve that when going beyond our simplified Z' setup. For instance, sticking only to R_K and R_{K^*} (so no angular observables, etc.), these can be accommodated via NP in electrons featuring sizeable contributions both from LH and RH quark currents, so that a negative contribution to ΔM_s is possible as well. This class of models were suggested in the context of Composite Higgs scenarios [81]. Alternatively, as pointed out in [82], in UV complete models of the vector lepto-quark $U_\mu \sim (3, 1, 2/3)$ [83–88] addressing both $R_{D^{(*)}}$ and $b \to s\ell\ell$ anomalies, the couplings to quarks of extra Z' and/or coloron states (not directly responsible for the anomalies in semi-leptonic B decays) can naturally have a large phase in order to accommodate a negative ΔM_s, without being in tension with CP violating observables. These two examples show that although it is difficult to obtain $\Delta M_s^{\text{NP}} < 0$ within simplified models for the $b \to s\ell\ell$ anomalies, that is certainly not impossible in more general constructions.

4 Conclusions

In this paper, we have combined recent results from sum rules [23, 24] (by some of the current authors, see also [20–22] for consistent results for the operator Q_1 by a different group), and the FNAL/MILC [12] and HPQCD [25] lattice collaborations into updated

JHEP12(2019)009

predictions for the mass differences

$$\Delta M_d^{\text{Average 2019}} = \left(0.533^{+0.022}_{-0.036}\right) \text{ps}^{-1} = \left(1.05^{+0.04}_{-0.07}\right) \Delta M_d^{\text{exp}} , \tag{4.1}$$

$$\Delta M_s^{\text{Average 2019}} = \left(18.4^{+0.7}_{-1.2}\right) \text{ps}^{-1} = \left(1.04^{+0.04}_{-0.07}\right) \Delta M_s^{\text{exp}} . \tag{4.2}$$

These results are about 40% more precise than the values in eq. (1.5) and eq. (1.6) obtained from the current FLAG [13] averages and show better agreement with the experimental results. The average for the SU(3)-breaking ratio ξ that determines the SM predictions for $\Delta M_d/\Delta M_s$ is dominated by the SR calculation combined with the most recent lattice results for the decay constants, which provides a precision much better than the lattice-alone value for this quantity. The new averages agree very well with the individual SR results (see figure 3 and figure 4), further reinforcing the usefulness of this as a totally independent determination of these important non-perturbative parameters. With our new average the hadronic uncertainties in these quantities are now at the same level as the CKM uncertainties. We then argued that with improved determinations of the hadronic matrix elements and the CKM elements the precision in ΔM_s can be improved to 3% by about 2025.

We investigated the constraints from ΔM_s on minimal Z' and LQ explanations of the $b \to s\ell\ell$ anomalies. The constraints for LQs are generally weaker because contributions to B_s mixing are only generated at loop level. Still we find that the assumed Future '25 scenario leads to an upper bound of 30 TeV on the LQ mass, stronger than the unitarity constraint [68, 69] by more than a factor of two. The situation for the Z' is summarized in figure 8. Despite the reduction of the uncertainty the constraints with the updated prediction Average '19 are *weaker* by about a factor $^3/_2$ than those obtained with the FLAG '19 scenario like in our earlier work [19] because of the smaller central value. Nevertheless, B_s mixing by itself is sufficient to exclude the minimal Z' scenario with a benchmark value of $\lambda^L_{22} = 1$ for the lepton coupling for Z' masses above 6 TeV. Assuming the Future '25 scenario, we obtain the upper limit $M_{Z'} \lesssim 9$ TeV for lepton couplings saturating the perturbativity bound (see right panel in figure 8), which is about six times better than the unitarity bound on the Z' mass. On the other hand, the left plot in figure 8 demonstrates that the parameter space will be very strongly constrained for more perturbative values of λ^L_{22}. An interesting open question is to what extent this mass window can be covered by direct searches at different future colliders.

Last but not least, we have addressed the question whether an extension of the minimal Z' scenario might relax the strong constraints. We have discussed two possibilities in which the minimal model might be extended, by adding new CP violating phases to the quark coupling, or including a coupling to both LH and RH quarks. For the case of new CP phases, the B_s mixing observable $A^{\text{CP}}_{\text{mix}}$ is very strongly constraining unless the real part is sufficiently small, which prevents an explanation of the anomalies. Adding instead a coupling to RH quarks has been recently discussed in the literature following the update, earlier this year at Moriond, of the LHCb measurement of R_K. We demonstrate that the currently observed pattern, with $R_{K^*} < R_K < 1$ requires a particular sign combination for the LH and RH quark couplings, which would lead to a positive shift to ΔM_s rather than a

JHEP12(2019)009

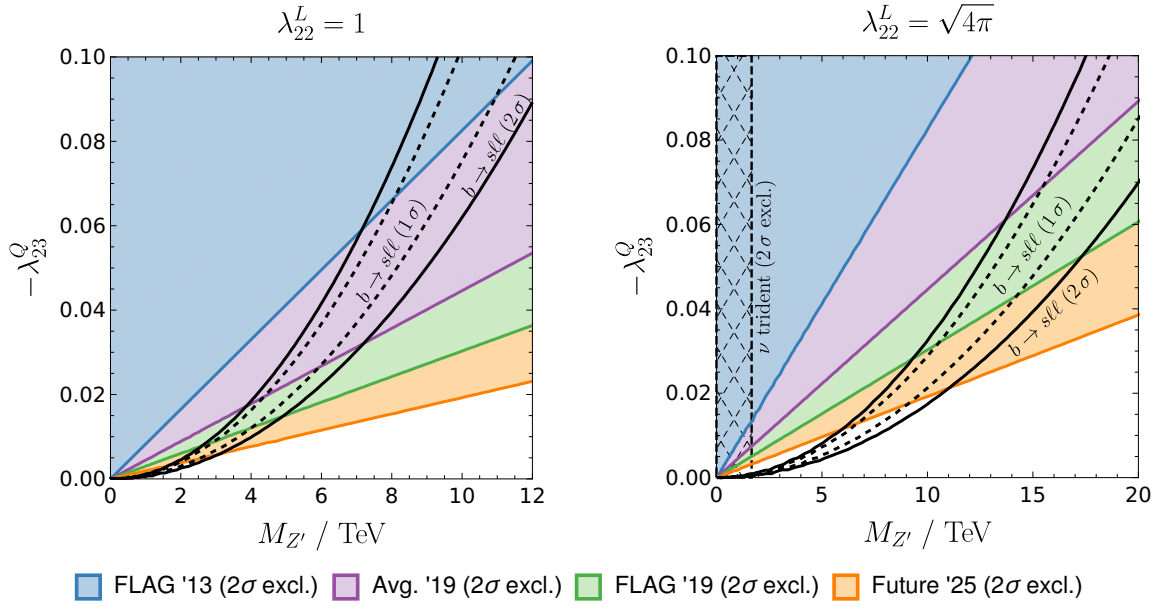

Figure 8. Parameter space of a naive Z' model explaining $b \to s\ell\ell$ via real LH currents, for two representative lepton couplings: $\lambda_{22}^L = 1$ (left panel) and $\lambda_{22}^L = \sqrt{4\pi}$ (right panel). Constraints from various determinations of ΔM_s and neutrino trident production are shown as well.

reduction. We conclude that the constraints from B_s mixing cannot be easily avoided within this class of minimally extended Z' simplified models, although more general constructions can achieve that.

All in all, we have shown how we are now entering the age of precision determinations of ΔM_s and that, as we proceed further, the latter will become an increasingly powerful tool in order to constrain new physics explanations of other flavour observables.

Acknowledgments

We thank Matheus Hostert for useful discussions. The work of LDL was supported by the ERC grant NEO-NAT. The work of AL is supported by the STFC grant of the IPPP. The work of MK was supported by MIUR (Italy) under a contract PRIN 2015P5SBHT and by INFN Sezione di Roma La Sapienza and partially supported by the ERC-2010 DaMESyFla Grant Agreement Number: 267985.

A Input parameters and average matrix elements

We list the input parameters required for the evaluation of the mass differences in table 2. We note that the CKM parameters are taken from the standard fit of the CKMfitter collaboration [75, 89] which includes ΔM_s and ΔM_d as constraints. The FNAL/MILC [12] and HPQCD [25] collaborations instead use the result of CKMfitter's tree fit

$$\text{tree fit: } V_{cb} = (42.41^{+0.40}_{-1.51}) \times 10{-}3\,, \tag{A.1}$$

JHEP12(2019)009

Parameter	Value	Source
M_Z	$(91.1876 \pm 0.0021)\,\text{GeV}$	PDG 2019 [91, 92]
$\alpha_s(M_Z)$	0.1181 ± 0.0011	PDG 2019 [91, 92]
$m_{t,\text{pole}}$	$(173.1 \pm 0.9)\,\text{GeV}$	PDG 2019 [91, 92]
$\overline{m}_b(\overline{m}_b)$	$(4.18^{+0.03}_{-0.02})\,\text{GeV}$	PDG 2019 [91, 92]
V_{us}	$0.224745^{+0.000254}_{-0.000059}$	CKMfitter Summer 2018 [75, 89]
V_{ub}	$0.003746^{+0.000090}_{-0.000062}$	CKMfitter Summer 2018 [75, 89]
V_{cb}	$0.04240^{+0.00030}_{-0.00115}$	CKMfitter Summer 2018 [75, 89]
γ_{CKM}	$(65.81^{+0.99}_{-1.61})^\circ$	CKMfitter Summer 2018 [75, 89]
$\overline{m}_t(\overline{m}_t)$	$(163.3 \pm 0.9)\,\text{GeV}$	Own evaluation (RunDec [93, 94])
f_{B_s}	$(230.3 \pm 1.3)\,\text{MeV}$	FLAG 2019 [13]
f_B	$(190.0 \pm 1.3)\,\text{MeV}$	FLAG 2019 [13]

Table 2. Input parameters for our calculations of ΔM_s and ΔM_d.

which uses only tree-level observables and is therefore independent of the mass differences. However, also a number of other observables are discarded in this approach. Using CKMlive [90] we have performed a fit where only ΔM_s and ΔM_d were excluded which yields

$$\text{fit without } \Delta M_{s,d}\text{: } V_{cb} = (42.40^{+0.40}_{-1.17}) \times 10{-}3\,. \tag{A.2}$$

We observe that this result is very close to that from the standard fit shown in table 2 and therefore use the standard fit for simplicity.

In addition to our averages given in eq. (2.8) we also provide the weighted averages for the matrix elements in the B_d system

$$\begin{aligned}
f_B^2 B_1^d(\mu_b) &= (0.0305 \pm 0.0011)\,\text{GeV}^2\,,\\
f_B^2 B_2^d(\mu_b) &= (0.0288 \pm 0.0013)\,\text{GeV}^2\,,\\
f_B^2 B_3^d(\mu_b) &= (0.0281 \pm 0.0020)\,\text{GeV}^2\,,\\
f_B^2 B_4^d(\mu_b) &= (0.0387 \pm 0.0015)\,\text{GeV}^2\,,\\
f_B^2 B_5^d(\mu_b) &= (0.0361 \pm 0.0014)\,\text{GeV}^2\,,
\end{aligned} \tag{A.3}$$

and the weighted averages for the bag parameters

$$\begin{aligned}
B_1^s(\mu_b) &= 0.849 \pm 0.023\,, & B_1^d(\mu_b) &= 0.835 \pm 0.028\,,\\
B_2^s(\mu_b) &= 0.835 \pm 0.032\,, & B_2^d(\mu_b) &= 0.791 \pm 0.034\,,\\
B_3^s(\mu_b) &= 0.854 \pm 0.051\,, & B_3^d(\mu_b) &= 0.775 \pm 0.054\,,\\
B_4^s(\mu_b) &= 1.031 \pm 0.035\,, & B_4^d(\mu_b) &= 1.063 \pm 0.041\,,\\
B_5^s(\mu_b) &= 0.959 \pm 0.031\,, & B_5^d(\mu_b) &= 0.994 \pm 0.037\,,
\end{aligned} \tag{A.4}$$

at the scale $\mu_b = \bar{m}_b(\bar{m}_b)$.

JHEP12(2019)009

References

[1] M. Artuso, G. Borissov and A. Lenz, *CP violation in the B_s^0 system*, *Rev. Mod. Phys.* **88** (2016) 045002 [arXiv:1511.09466] [INSPIRE].

[2] HFLAV collaboration, *Averages of b-hadron, c-hadron and τ-lepton properties as of summer 2016*, *Eur. Phys. J.* **C 77** (2017) 895 [arXiv:1612.07233] [INSPIRE].

[3] ARGUS collaboration, *Observation of B^0-$\bar{B}^0$ Mixing*, *Phys. Lett.* **B 192** (1987) 245 [INSPIRE].

[4] CDF collaboration, *Observation of B_s^0-$\bar{B}_s^0$ Oscillations*, *Phys. Rev. Lett.* **97** (2006) 242003 [hep-ex/0609040] [INSPIRE].

[5] LHCb collaboration, *Measurement of the B_s^0-$\bar{B}_s^0$ oscillation frequency Δm_s in $B_s^0 \to D_s^-(3)\pi$ decays*, *Phys. Lett.* **B 709** (2012) 177 [arXiv:1112.4311] [INSPIRE].

[6] LHCb collaboration, *Opposite-side flavour tagging of B mesons at the LHCb experiment*, *Eur. Phys. J.* **C 72** (2012) 2022 [arXiv:1202.4979] [INSPIRE].

[7] LHCb collaboration, *Measurement of the B^0-$\bar{B}^0$ oscillation frequency Δm_d with the decays $B^0 \to D^-\pi^+$ and $B^0 \to J/\psi K^{*0}$*, *Phys. Lett.* **B 719** (2013) 318 [arXiv:1210.6750] [INSPIRE].

[8] LHCb collaboration, *Precision measurement of the B_s^0-$\bar{B}_s^0$ oscillation frequency with the decay $B_s^0 \to D_s^-\pi^+$*, *New J. Phys.* **15** (2013) 053021 [arXiv:1304.4741] [INSPIRE].

[9] LHCb collaboration, *Observation of B_s^0-$\bar{B}_s^0$ mixing and measurement of mixing frequencies using semileptonic B decays*, *Eur. Phys. J.* **C 73** (2013) 2655 [arXiv:1308.1302] [INSPIRE].

[10] LHCb collaboration, *Precision measurement of CP violation in $B_s^0 \to J/\psi K^+K^-$ decays*, *Phys. Rev. Lett.* **114** (2015) 041801 [arXiv:1411.3104] [INSPIRE].

[11] S. Aoki et al., *Review of Lattice Results Concerning Low-Energy Particle Physics*, *Eur. Phys. J.* **C 74** (2014) 2890 [arXiv:1310.8555] [INSPIRE].

[12] Fermilab Lattice and MILC collaborations, *$B_{(s)}^0$-mixing matrix elements from lattice QCD for the Standard Model and beyond*, *Phys. Rev.* **D 93** (2016) 113016 [arXiv:1602.03560] [INSPIRE].

[13] Flavour Lattice Averaging Group collaboration, *FLAG Review 2019*, arXiv:1902.08191 [INSPIRE].

[14] M. Blanke and A.J. Buras, *Universal Unitarity Triangle 2016 and the tension between $\Delta M_{s,d}$ and ε_K in CMFV models*, *Eur. Phys. J.* **C 76** (2016) 197 [arXiv:1602.04020] [INSPIRE].

[15] A.J. Buras and F. De Fazio, *331 Models Facing the Tensions in $\Delta F = 2$ Processes with the Impact on ε'/ε, $B_s \to \mu^+\mu^-$ and $B \to K^*\mu^+\mu^-$*, *JHEP* **08** (2016) 115 [arXiv:1604.02344] [INSPIRE].

[16] C. Bobeth, A.J. Buras, A. Celis and M. Jung, *Yukawa enhancement of Z-mediated new physics in $\Delta S = 2$ and $\Delta B = 2$ processes*, *JHEP* **07** (2017) 124 [arXiv:1703.04753] [INSPIRE].

JHEP12(2019)009

[17] M. Blanke and A.J. Buras, *Emerging ΔM_d-anomaly from tree-level determinations of $|V_{cb}|$ and the angle γ*, *Eur. Phys. J.* **C 79** (2019) 159 [arXiv:1812.06963] [INSPIRE].

[18] Q.-Y. Hu, X.-Q. Li, Y.-D. Yang and M.-D. Zheng, *$B_{s(d)} - \bar{B}_{s(d)}$ Mixing and $B_s \to \mu^+\mu^-$ Decay in the NMSSM with the Flavour Expansion Theorem*, *JHEP* **06** (2019) 133 [arXiv:1903.06927] [INSPIRE].

[19] L. Di Luzio, M. Kirk and A. Lenz, *Updated B_s-mixing constraints on new physics models for $b \to s\ell^+\ell^-$ anomalies*, *Phys. Rev.* **D 97** (2018) 095035 [arXiv:1712.06572] [INSPIRE].

[20] A.G. Grozin, R. Klein, T. Mannel and A.A. Pivovarov, *B^0-$\bar{B}^0$ mixing at next-to-leading order*, *Phys. Rev.* **D 94** (2016) 034024 [arXiv:1606.06054] [INSPIRE].

[21] A.G. Grozin, T. Mannel and A.A. Pivovarov, *Towards a Next-to-Next-to-Leading Order analysis of matching in B^0-$\bar{B}^0$ mixing*, *Phys. Rev.* **D 96** (2017) 074032 [arXiv:1706.05910] [INSPIRE].

[22] A.G. Grozin, T. Mannel and A.A. Pivovarov, *B^0-$\bar{B}^0$ mixing: Matching to HQET at NNLO*, *Phys. Rev.* **D 98** (2018) 054020 [arXiv:1806.00253] [INSPIRE].

[23] M. Kirk, A. Lenz and T. Rauh, *Dimension-six matrix elements for meson mixing and lifetimes from sum rules*, *JHEP* **12** (2017) 068 [arXiv:1711.02100] [INSPIRE].

[24] D. King, A. Lenz and T. Rauh, *B_s mixing observables and $|V_{td}/V_{ts}|$ from sum rules*, *JHEP* **05** (2019) 034 [arXiv:1904.00940] [INSPIRE].

[25] R.J. Dowdall et al., *Neutral B-meson mixing from full lattice QCD at the physical point*, arXiv:1907.01025 [INSPIRE].

[26] RBC/UKQCD collaboration, *SU(3)-breaking ratios for $D_{(s)}$ and $B_{(s)}$ mesons*, arXiv:1812.08791 [INSPIRE].

[27] BELLE-II collaboration, *The Belle II Physics Book*, arXiv:1808.10567 [INSPIRE].

[28] LHCb collaboration, *Physics case for an LHCb Upgrade II — Opportunities in flavour physics and beyond, in the HL-LHC era*, arXiv:1808.08865 [INSPIRE].

[29] T. Inami and C.S. Lim, *Effects of Superheavy Quarks and Leptons in Low-Energy Weak Processes $L_L \to \mu\bar{\mu}$, $K^+ \to \pi^+\nu\bar{\nu}$ and $K^0 \leftrightarrow \bar{K}^0$*, *Prog. Theor. Phys.* **65** (1981) 297 [*Erratum ibid.* **65** (1981) 1772] [INSPIRE].

[30] A.J. Buras, M. Jamin and P.H. Weisz, *Leading and Next-to-leading QCD Corrections to ϵ Parameter and B^0-$\bar{B}^0$ Mixing in the Presence of a Heavy Top Quark*, *Nucl. Phys.* **B 347** (1990) 491 [INSPIRE].

[31] ETM collaboration, *B-physics from $N_f = 2$ tmQCD: the Standard Model and beyond*, *JHEP* **03** (2014) 016 [arXiv:1308.1851] [INSPIRE].

[32] ETM collaboration, *Mass of the b quark and B-meson decay constants from $N_f = 2+1+1$ twisted-mass lattice QCD*, *Phys. Rev.* **D 93** (2016) 114505 [arXiv:1603.04306] [INSPIRE].

[33] C. Hughes, C.T.H. Davies and C.J. Monahan, *New methods for B meson decay constants and form factors from lattice NRQCD*, *Phys. Rev.* **D 97** (2018) 054509 [arXiv:1711.09981] [INSPIRE].

[34] A. Bazavov et al., *B- and D-meson leptonic decay constants from four-flavor lattice QCD*, *Phys. Rev.* **D 98** (2018) 074512 [arXiv:1712.09262] [INSPIRE].

[35] A.G. Grozin and R.N. Lee, *Three-loop HQET vertex diagrams for B^0-$\bar{B}^0$ mixing*, *JHEP* **02** (2009) 047 [arXiv:0812.4522] [INSPIRE].

JHEP12(2019)009

[36] RBC/UKQCD collaboration, *Neutral Kaon Mixing Beyond the Standard Model with $n_f = 2 + 1$ Chiral Fermions Part 1: Bare Matrix Elements and Physical Results*, *JHEP* **11** (2016) 001 [arXiv:1609.03334] [INSPIRE].

[37] A. Cerri et al., *Opportunities in Flavour Physics at the HL-LHC and HE-LHC*, arXiv:1812.07638 [INSPIRE].

[38] J.G. Korner, A.I. Onishchenko, A.A. Petrov and A.A. Pivovarov, *B^0-$\bar{B}^0$ mixing beyond factorization*, *Phys. Rev. Lett.* **91** (2003) 192002 [hep-ph/0306032] [INSPIRE].

[39] T. Mannel, B.D. Pecjak and A.A. Pivovarov, *Sum rule estimate of the subleading non-perturbative contributions to B_s-$\bar{B}_s$ mixing*, *Eur. Phys. J.* **C 71** (2011) 1607 [hep-ph/0703244] [INSPIRE].

[40] LHCb collaboration, *Test of lepton universality using $B^+ \to K^+\ell^+\ell^-$ decays*, *Phys. Rev. Lett.* **113** (2014) 151601 [arXiv:1406.6482] [INSPIRE].

[41] LHCb collaboration, *Test of lepton universality with $B^0 \to K^{*0}\ell^+\ell^-$ decays*, *JHEP* **08** (2017) 055 [arXiv:1705.05802] [INSPIRE].

[42] LHCb collaboration, *Search for lepton-universality violation in $B^+ \to K^+\ell^+\ell^-$ decays*, *Phys. Rev. Lett.* **122** (2019) 191801 [arXiv:1903.09252] [INSPIRE].

[43] LHCb collaboration, *Angular analysis and differential branching fraction of the decay $B_s^0 \to \phi\mu^+\mu^-$*, *JHEP* **09** (2015) 179 [arXiv:1506.08777] [INSPIRE].

[44] CMS collaboration, *Angular analysis of the decay $B^0 \to K^{*0}\mu^+\mu^-$ from pp collisions at $\sqrt{s} = 8$ TeV*, *Phys. Lett.* **B 753** (2016) 424 [arXiv:1507.08126] [INSPIRE].

[45] BABAR collaboration, *Measurement of angular asymmetries in the decays $B \to K^*\ell^+\ell^-$*, *Phys. Rev.* **D 93** (2016) 052015 [arXiv:1508.07960] [INSPIRE].

[46] BELLE collaboration, *Measurement of the Differential Branching Fraction and Forward-Backword Asymmetry for $B \to K^{(*)}\ell^+\ell^-$*, *Phys. Rev. Lett.* **103** (2009) 171801 [arXiv:0904.0770] [INSPIRE].

[47] CDF collaboration, *Measurements of the Angular Distributions in the Decays $B \to K^{(*)}\mu^+\mu^-$ at CDF*, *Phys. Rev. Lett.* **108** (2012) 081807 [arXiv:1108.0695] [INSPIRE].

[48] LHCb collaboration, *Angular analysis of the $B^0 \to K^{*0}\mu^+\mu^-$ decay using $3\,fb^{-1}$ of integrated luminosity*, *JHEP* **02** (2016) 104 [arXiv:1512.04442] [INSPIRE].

[49] BELLE collaboration, *Angular analysis of $B^0 \to K^*(892)^0\ell^+\ell^-$*, in *Proceedings, LHCSki 2016 — A First Discussion of 13 TeV Results*, Obergurgl, Austria, 10–15 April 2016 (2016) [arXiv:1604.04042] [INSPIRE].

[50] BELLE collaboration, *Lepton-Flavor-Dependent Angular Analysis of $B \to K^*\ell^+\ell^-$*, *Phys. Rev. Lett.* **118** (2017) 111801 [arXiv:1612.05014] [INSPIRE].

[51] CMS collaboration, *Measurement of angular parameters from the decay $\mathrm{B}^0 \to \mathrm{K}^{*0}\mu^+\mu^-$ in proton-proton collisions at $\sqrt{s} = 8$ TeV*, *Phys. Lett.* **B 781** (2018) 517 [arXiv:1710.02846] [INSPIRE].

[52] ATLAS collaboration, *Angular analysis of $B_d^0 \to K^*\mu^+\mu^-$ decays in pp collisions at $\sqrt{s} = 8$ TeV with the ATLAS detector*, *JHEP* **10** (2018) 047 [arXiv:1805.04000] [INSPIRE].

[53] LHCb collaboration, *Differential branching fractions and isospin asymmetries of $B \to K^{(*)}\mu^+\mu^-$ decays*, *JHEP* **06** (2014) 133 [arXiv:1403.8044] [INSPIRE].

JHEP12(2019)009

[54] J. Aebischer, W. Altmannshofer, D. Guadagnoli, M. Reboud, P. Stangl and D.M. Straub, *B-decay discrepancies after Moriond 2019*, arXiv:1903.10434 [INSPIRE].

[55] M. Algueró et al., *Emerging patterns of New Physics with and without Lepton Flavour Universal contributions*, *Eur. Phys. J.* **C 79** (2019) 714 [arXiv:1903.09578] [INSPIRE].

[56] K. Kowalska, D. Kumar and E.M. Sessolo, *Implications for new physics in $b \to s\mu\mu$ transitions after recent measurements by Belle and LHCb*, *Eur. Phys. J.* **C 79** (2019) 840 [arXiv:1903.10932] [INSPIRE].

[57] M. Ciuchini et al., *New Physics in $b \to s\ell^+\ell^-$ confronts new data on Lepton Universality*, *Eur. Phys. J.* **C 79** (2019) 719 [arXiv:1903.09632] [INSPIRE].

[58] P. Arnan, A. Crivellin, M. Fedele and F. Mescia, *Generic loop effects of new scalars and fermions in $b \to s\ell^+\ell^-$ and a vector-like 4^{th} generation*, *JHEP* **06** (2019) 118 [arXiv:1904.05890] [INSPIRE].

[59] G. D'Amico et al., *Flavour anomalies after the R_{K^*} measurement*, *JHEP* **09** (2017) 010 [arXiv:1704.05438] [INSPIRE].

[60] A.K. Alok, A. Dighe, S. Gangal and D. Kumar, *Continuing search for new physics in $b \to s\mu\mu$ decays: two operators at a time*, *JHEP* **06** (2019) 089 [arXiv:1903.09617] [INSPIRE].

[61] J.A. Bagger, K.T. Matchev and R.-J. Zhang, *QCD corrections to flavor changing neutral currents in the supersymmetric standard model*, *Phys. Lett.* **B 412** (1997) 77 [hep-ph/9707225] [INSPIRE].

[62] I. Doršner, S. Fajfer, A. Greljo, J.F. Kamenik and N. Košnik, *Physics of leptoquarks in precision experiments and at particle colliders*, *Phys. Rept.* **641** (2016) 1 [arXiv:1603.04993] [INSPIRE].

[63] W. Altmannshofer, S. Gori, J. Martín-Albo, A. Sousa and M. Wallbank, *Neutrino Tridents at DUNE*, arXiv:1902.06765 [INSPIRE].

[64] CCFR collaboration, *Neutrino tridents and W Z interference*, *Phys. Rev. Lett.* **66** (1991) 3117 [INSPIRE].

[65] DUNE collaboration, *The DUNE Far Detector Interim Design Report Volume 1: Physics, Technology and Strategies*, arXiv:1807.10334 [INSPIRE].

[66] ATLAS collaboration, *Search for new high-mass phenomena in the dilepton final state using $36\,fb^{-1}$ of proton-proton collision data at $\sqrt{s} = 13\,TeV$ with the ATLAS detector*, *JHEP* **10** (2017) 182 [arXiv:1707.02424] [INSPIRE].

[67] CMS collaboration, *Search for third-generation scalar leptoquarks and heavy right-handed neutrinos in final states with two tau leptons and two jets in proton-proton collisions at $\sqrt{s} = 13\,TeV$*, *JHEP* **07** (2017) 121 [arXiv:1703.03995] [INSPIRE].

[68] L. Di Luzio and M. Nardecchia, *What is the scale of new physics behind the B-flavour anomalies?*, *Eur. Phys. J.* **C 77** (2017) 536 [arXiv:1706.01868] [INSPIRE].

[69] L. Di Luzio, J.F. Kamenik and M. Nardecchia, *Implications of perturbative unitarity for scalar di-boson resonance searches at LHC*, *Eur. Phys. J.* **C 77** (2017) 30 [arXiv:1604.05746] [INSPIRE].

[70] B.C. Allanach, B. Gripaios and T. You, *The case for future hadron colliders from $B \to K^{(*)}\mu^+\mu^-$ decays*, *JHEP* **03** (2018) 021 [arXiv:1710.06363] [INSPIRE].

JHEP12(2019)009

[71] Y. Afik, J. Cohen, E. Gozani, E. Kajomovitz and Y. Rozen, *Establishing a Search for $b \to s\ell^+\ell^-$ Anomalies at the LHC*, *JHEP* **08** (2018) 056 [arXiv:1805.11402] [INSPIRE].

[72] L. Di Luzio, M. Kirk and A. Lenz, *B_s-$\bar{B}_s$ mixing interplay with B anomalies*, in *10th International Workshop on the CKM Unitarity Triangle (CKM 2018)*, Heidelberg, Germany, 17–21 September 2018 (2018) [arXiv:1811.12884] [INSPIRE].

[73] A. Lenz and U. Nierste, *Theoretical update of B_s-$\bar{B}_s$ mixing*, *JHEP* **06** (2007) 072 [hep-ph/0612167] [INSPIRE].

[74] HFLAV collaboration, *HFLAV PDG 2018 results*, http://www.slac.stanford.edu/xorg/hflav/osc/PDG_2018/.

[75] CKMFITTER collaboration, *CKMfitter Summer 2018 results*, http://ckmfitter.in2p3.fr/www/results/plots_summer18/ckm_res_summer18.html.

[76] A.K. Alok, B. Bhattacharya, D. Kumar, J. Kumar, D. London and S.U. Sankar, *New physics in $b \to s\mu^+\mu^-$: Distinguishing models through CP-violating effects*, *Phys. Rev.* **D 96** (2017) 015034 [arXiv:1703.09247] [INSPIRE].

[77] J. Alda, J. Guasch and S. Penaranda, *Some results on Lepton Flavour Universality Violation*, *Eur. Phys. J.* **C 79** (2019) 588 [arXiv:1805.03636] [INSPIRE].

[78] D.M. Straub, *flavio: a Python package for flavour and precision phenomenology in the Standard Model and beyond*, arXiv:1810.08132 [INSPIRE].

[79] W. Altmannshofer, C. Niehoff, P. Stangl and D.M. Straub, *Status of the $B \to K^*\mu^+\mu^-$ anomaly after Moriond 2017*, *Eur. Phys. J.* **C 77** (2017) 377 [arXiv:1703.09189] [INSPIRE].

[80] G. Hiller and M. Schmaltz, *Diagnosing lepton-nonuniversality in $b \to s\ell\ell$*, *JHEP* **02** (2015) 055 [arXiv:1411.4773] [INSPIRE].

[81] A. Carmona and F. Goertz, *Recent B physics anomalies: a first hint for compositeness?*, *Eur. Phys. J.* **C 78** (2018) 979 [arXiv:1712.02536] [INSPIRE].

[82] M. Bordone, C. Cornella, J. Fuentes-Martín and G. Isidori, *Low-energy signatures of the* PS^3 *model: from B-physics anomalies to LFV*, *JHEP* **10** (2018) 148 [arXiv:1805.09328] [INSPIRE].

[83] L. Di Luzio, A. Greljo and M. Nardecchia, *Gauge leptoquark as the origin of B-physics anomalies*, *Phys. Rev.* **D 96** (2017) 115011 [arXiv:1708.08450] [INSPIRE].

[84] L. Calibbi, A. Crivellin and T. Li, *Model of vector leptoquarks in view of the B-physics anomalies*, *Phys. Rev.* **D 98** (2018) 115002 [arXiv:1709.00692] [INSPIRE].

[85] M. Bordone, C. Cornella, J. Fuentes-Martin and G. Isidori, *A three-site gauge model for flavor hierarchies and flavor anomalies*, *Phys. Lett.* **B 779** (2018) 317 [arXiv:1712.01368] [INSPIRE].

[86] R. Barbieri and A. Tesi, *B-decay anomalies in Pati-Salam* SU(4), *Eur. Phys. J.* **C 78** (2018) 193 [arXiv:1712.06844] [INSPIRE].

[87] M. Blanke and A. Crivellin, *B Meson Anomalies in a Pati-Salam Model within the Randall-Sundrum Background*, *Phys. Rev. Lett.* **121** (2018) 011801 [arXiv:1801.07256] [INSPIRE].

[88] L. Di Luzio, J. Fuentes-Martin, A. Greljo, M. Nardecchia and S. Renner, *Maximal Flavour Violation: a Cabibbo mechanism for leptoquarks*, *JHEP* **11** (2018) 081 [arXiv:1808.00942] [INSPIRE].

JHEP12(2019)009

[89] CKMfitter Group collaboration, *CP violation and the CKM matrix: Assessing the impact of the asymmetric B factories*, *Eur. Phys. J.* **C 41** (2005) 1 [hep-ph/0406184] [INSPIRE].

[90] CKMfitter collaboration, *CKMlive*, http://ckmlive.in2p3.fr.

[91] Particle Data Group collaboration, *Review of Particle Physics*, *Phys. Rev.* **D 98** (2018) 030001 [INSPIRE].

[92] Particle Data Group collaboration, *PDG 2019 update*, http://pdg.lbl.gov/.

[93] K.G. Chetyrkin, J.H. Kuhn and M. Steinhauser, *RunDec: A Mathematica package for running and decoupling of the strong coupling and quark masses*, *Comput. Phys. Commun.* **133** (2000) 43 [hep-ph/0004189] [INSPIRE].

[94] F. Herren and M. Steinhauser, *Version 3 of RunDec and CRunDec*, *Comput. Phys. Commun.* **224** (2018) 333 [arXiv:1703.03751] [INSPIRE].

JHEP12(2019)009